THE JOURNAL OF BIOLOGICAL CHEMISTRY VOL. 285, NO. 15, pp. 11143–11153, April 9, 2010

Neurologic Dysfunction and Male Infertility in *Drosophila porin* Mutants

A NEW MODEL FOR MITOCHONDRIAL DYSFUNCTION AND DISEASE[*] [S]

Received for publication, October 28, 2009, and in revised form, January 8, 2010 Published, JBC Papers in Press, January 28, 2010, DOI 10.1074/jbc.M109.080317

Brett H. Graham[‡1], Zhihong Li[‡], Erminio P. Alesii[‡], Patrik Versteken[§¶], Cynthia Lee[‡], Jennifer Wang[‡], and William J. Craigen[‡‖]

From the Departments of [‡]Molecular and Human Genetics and [‖]Pediatrics, Baylor College of Medicine, Houston, Texas 77030 and the [§]VIB Department of Molecular and Developmental Genetics and [¶]Center for Human Genetics, Katholieke Universiteit Leuven, 3000 Leuven, Belgium

Voltage-dependent anion channels (VDACs) are a family of small pore-forming proteins of the mitochondrial outer membrane found in all eukaryotes. VDACs play an important role in the regulated flux of metabolites between the cytosolic and mitochondrial compartments, and three distinct mammalian isoforms have been identified. Animal and cell culture experiments suggest that the various isoforms act in disparate roles such as apoptosis, synaptic plasticity, learning, muscle bioenergetics, and reproduction. In *Drosophila melanogaster*, *porin* is the ubiquitously expressed VDAC isoform. Through imprecise excision of a P element insertion in the *porin* locus, a series of hypomorphic alleles have been isolated, and analyses of flies homozygous for these mutant alleles reveal phenotypes remarkably reminiscent of mouse VDAC mutants. These include partial lethality, defects of mitochondrial respiration, abnormal muscle mitochondrial morphology, synaptic dysfunction, and male infertility, which are features often observed in human mitochondrial disorders. Furthermore, the observed synaptic dysfunction at the neuromuscular junction in *porin* mutants is associated with a paucity of mitochondria in presynaptic termini. The similarity of VDAC mutant phenotypes in the fly and mouse clearly indicate a fundamental conservation of VDAC function. The establishment and validation of a new *in vivo* model for VDAC function in *Drosophila* should provide a valuable tool for further genetic dissection of VDAC role(s) in mitochondrial biology and disease, and as a model of mitochondrial disorders potentially amenable to the development of treatment strategies.

The voltage-dependent anion channel (VDAC)[2] is an integral membrane protein present in the mitochondrial outer membrane. VDAC is a monomeric, voltage-gated channel that allows passage of molecules up to 5,000 daltons (1), and multiple isoforms have been identified in numerous eukaryotic species (2–5). VDAC provides the predominant pathway for small metabolites such as ATP, ADP, phosphocreatine and small ions across the mitochondrial outer membrane (1, 6). The mechanism of channel permeation appears to reflect large changes in protein conformation and channel charge rather than a physical restriction to ion flow (7). In addition to its role in energy metabolism, VDAC has been implicated in various basic cellular and developmental processes such as cytochrome *c*-dependent apoptosis (8, 9) and the mitochondrial permeability transition pore (10, 11). These potential roles in fundamental cellular activities underscore the importance of elucidating VDAC biological functions to better understand mitochondrial functions.

Studies in mammalian model systems have detected functional differences in various VDAC isoforms. Mice deficient for *Vdac1* and *Vdac3* have distinct phenotypes, with $Vdac1^{-/-}$ mice exhibiting partial embryonic lethality (11), as well as abnormal respiratory chain activities and mitochondrial morphology in muscle (12). $Vdac3^{-/-}$ mice demonstrate sperm motility defects and, similarly, abnormal respiratory chain activities and mitochondrial morphology in muscle (13). In addition, $Vdac1^{-/-}$, $Vdac3^{-/-}$, and $Vdac1/3^{-/-}$ double mutants all exhibit defects in associative and spatial learning that correlate with electrophysiological deficits in synaptic plasticity (11). Despite these studies implicating VDAC in neuromuscular function and spermatogenesis, the specific cellular and developmental roles of the various VDAC isoforms, as well as the proteins or pathways with which VDACs interact, are not yet well understood. The use of genetic model systems such as *Drosophila melanogaster* offers the possibility of gaining additional *in vivo* insights into VDAC functions, its intracellular interactions, and its potential as a therapeutic target.

D. melanogaster contains a cluster of four genes (*porin*, *CG17137* (*Porin2*), *CG17139*, and *CG17140*) that encode pro-

* This work was supported, in whole or in part, by National Institutes of Health Grants K08 HD44808 (to B. H. G.) and R01 NS0423193 (to W. J. C.). This work was also supported by March of Dimes FY-99-323 (to W. J. C.), Fund for Scientific Research Flanders (FWO, G.0747.09) (to P. V.), Research Fund Katholieke Universiteit Leuven (P. V.), a Marie Curie Excellence Grant (MEXT-CT-2006-042267) (to P. V.), The Baylor College of Medicine Mental Retardation Developmental Disabilities Research Center (MRDDRC HD024064), and VIB (to P. V.).

[S] The on-line version of this article (available at http://www.jbc.org) contains supplemental "Experimental Procedures," Tables S1 and S2, Figs. S1–S3, and additional references.

[1] Recipient of The Baylor College of Medicine Children's Health Research Center Scholar Grant (National Institutes of Health Grant 5K12 DH41648) and the American Academy of Pediatrics (Section on Genetics and Birth Defects) 2003 Young Investigator Research Grant. To whom correspondence should be addressed: Rm. T536, BCM225, One Baylor Plaza, Houston, TX 77030. Fax: 713-798-1445; E-mail: bgraham@bcm.edu.

[2] The abbreviations used are: VDAC, voltage-dependent anion channel; CNS, central nervous system; NMJ, neuromuscular junction; mitoGFP, mitochondrial-targeted GFP; ERG, electroretinogram; EJP, excitatory junctional potential.

teins that are homologous to known VDACs (14–16). *porin* exhibits the greatest homology to mammalian VDACs and is ubiquitously expressed in the fruit fly, whereas the other three fly VDACs have a more spatially restricted expression pattern and are predominantly present in the male reproductive tract (17). When expressed in VDAC-deficient yeast, *porin* and *CG17137* can rescue a conditional lethal phenotype, whereas the other two cannot, demonstrating functional complementation for a subset of these genes (7). Given its homology to mammalian VDACs and its ubiquitous expression pattern, it was hypothesized that *porin* represents the predominant functional ortholog of VDAC in *Drosophila*. This hypothesis predicts that mutant *porin* phenotypes should exhibit significant similarities to mammalian mutant VDAC phenotypes. In this study, analysis of mutant *porin* phenotypes reveals a striking concordance with mammalian mutant VDAC phenotypes. In addition, the demonstration of a secondary respiratory chain deficiency and abnormal distribution of mitochondria within motor neurons of *porin* mutants provides new insights into the phenotypic consequences of VDAC deficiency, illustrating the potential of *Drosophila* as a useful model system to study mitochondrial function and disease.

EXPERIMENTAL PROCEDURES

Fly Stocks—Unless mentioned elsewhere, all primary stocks described were obtained from the Bloomington *Drosophila* Stock Center. All stocks were maintained at room temperature using standard cornmeal-molasses-yeast media. "*yw*" indicates the genotype $y^1\ w^{67c23}$.

P Element Excision—The P element line *y w*; $porin^{EY2333}$ (18) was crossed to *y w*; *L*/*CyO*; $K_{i1}\ \Delta 2\text{–}3$ (provided by Hugo Bellen, Baylor College of Medicine) to induce excisions, and 400 lines were generated. One allele, $porin^{Rev8}$ failed to complement $porin^{l(2)k05123}$ (19) and was balanced over *SM6b*. Long range PCR demonstrates that this imprecise excision event results in an insertion of ~7 kb (supplemental Fig. S1*C*). Three other alleles ($porin^{Ex75}$, $porin^{Ex78}$, and $porin^{Ex365}$) were identified as deletions from imprecise excisions by PCR analysis, and the breakpoints identified by DNA sequencing of the deletion junction fragments. In addition, two other alleles ($porin^{Ex341}$ and $porin^{ExS27}$) were established as independent precise excision controls and verified by DNA sequencing across the parental P element insertion site (supplemental Fig. S1).

Transgenic Rescue—A cDNA (from Berkley *Drosophila* Genome Project clone GM13853) (17) containing the wild type full coding sequence of *porin* was cloned into the P element transformation vector pUAST and injected into *yw* embryos; transgenic lines were established, and ectopic wild type *porin* was expressed in *porin* mutant background using the *GAL4*-UAS system (20). The *GAL4* drivers were the ubiquitous *Tubulin-GAL4* (21), the neuronal *ELAV-GAL4* (22), and c135-*GAL4*, which is expressed in the male reproductive tract (23).

Molecular Biology—Whole fly lysates or dissected testes lysates were used for Western blot analyses that were performed as described previously (17).

Lifespan Analysis—For measuring lifespan, flies of indicated genotypes were isolated on the day of eclosion and placed into same-sex cohorts of five flies per vial. Each day the number of surviving flies was recorded until all flies had died. The flies were placed in fresh vials three times per week (Monday, Wednesday, and Friday) during the entire test.

Mitochondrial Polarography and Enzymology—Polarographic experiments were performed as described previously (24) with the following changes. Intact mitochondria were isolated by differential centrifugation from fresh homogenates of three-day-old adult flies, with the homogenates first filtered through cheesecloth to remove residual particulate remains of the exoskeleton. Oxygen consumption of mitochondria was measured in a 650-μl chamber fitted with a Clark microelectrode (YSI Life Sciences), recorded using a PowerLab electronic data recorder, and analyzed using LabChart (AD Instruments).

For enzymologic assays of respiratory chain complexes I–IV, sufficient third instar larval stage larvae were collected to fill a 1.5-ml Eppendorf tube to 50 μl. Potassium phosphate buffer (25 mM, pH 7.5) was added to a final volume of 300 μl, and the larvae were sonicated (5-s pulse ×4, 60% power) using a Microson XL2000 Ultrasonic Cell Disruptor (Misonix). The spectrophotometric kinetic assays were performed at 30 °C in a volume of 100 μl using a monochromator microplate reader (Tecan M200). Complex I activity (NADH:ubiquinone oxidoreductase) was determined by measuring oxidation of NADH at 340 nm (using ferricyanide as the electron acceptor) in a reaction mixture of 25 mM potassium phosphate (pH 7.5), 0.2 mM NADH, and 1.7 mM potassium ferricyanide. Complex II activity (succinate dehydrogenase) was determined by measuring the reduction of the artificial electron acceptor 2,6-dichlorophenol-indophenol at 600 nm in a reaction mixture of 25 mM potassium phosphate (pH 7.5), 20 mM succinate, 0.5 mM 2,6-dichlorophenol-indophenol, 10 μM rotenone, 2 μg/ml antimycin A, and 2 mM potassium cyanide. Complex III activity (ubiquinol: cytochrome *c* oxidoreductase) was determined by measuring the reduction of cytochrome *c* at 550 nm in a reaction mixture of 25 mM potassium phosphate (pH 7.5), 35 μM reduced decylubiquinone, 15 μM cytochrome *c*, 10 μM rotenone, and 2 mM potassium cyanide. Complex IV activity (cytochrome *c* oxidase) was determined by measuring the oxidation of cytochrome *c* at 550 nm in a reaction mixture of 10 mM potassium phosphate (pH 7.5) and 0.1 mM reduced cytochrome *c*. Citrate synthase activity was determined by measuring the reduction of 5,5′-dithiobis(2-nitrobenzoic acid) at 412 nm, which is coupled to the reduction of acetyl-CoA by citrate synthase in the presence of oxaloacetate. The reaction mixture consists of 10 mM potassium phosphate (pH 7.5), 100 μM 5,5′-dithiobis(2-nitrobenzoic acid), 50 μM acetyl-CoA, and 250 μM oxaloacetate. All activities were calculated as nmol/min/mg protein, normalized to citrate synthase activity and expressed as a percentage of wild type activity.

Transmission Electron Microscopy—For transmission electron microscopy of indirect flight muscle, the indirect flight muscle of 7-day-old flies was dissected in ice-cold 4% paraformaldehyde/1% glutaraldehyde/0.1 M cacodylic acid (pH 7.2). Fixation, post-fixation, staining, embedding, sectioning, and transmission electron microscopy were performed as described previously (25).

Fertility and Fecundity Tests—For male fertility tests, individual 3-day-old males of the indicated genotypes were mated with two virgin *yw* females. After 3 days, each vial was visually examined to ensure eggs had been laid and the parents were discarded. After 17 days (from the initial mating), the total number of adult progeny was recorded. A minimum of 20 males for each genotype was used for testing. For female fecundity and fertility tests, individual virgin females of the indicated genotypes were paired with single virgin *yw* males. For 21 consecutive days, each mating pair was transferred to a fresh vial. The vial from the previous 24-h period was visually inspected and the total number of eggs laid was recorded and summed over the 21-day period. Each vial was also saved for 17 days, and then the total number of adult progeny was recorded and summed over the 21-day period. From these data, the total number of eggs laid, the total number of adult progeny, and the ratio of total progeny to total number of eggs laid were determined. Ten females of each genotype were tested to obtain mean values for the above parameters.

Measurement of Testis Width—Testes from 3-day-old males of each indicated genotype were dissected in 1× phosphate-buffered saline and photographed using a Leica S8 stereomicroscope fitted with a Leica DC300 digital camera (Meyer Instruments). Images were captured using Leica IM50 image management software. An image of a ruler (1-mm units) at the same magnification as the testes (80×) was photographed to provide reference for measuring the absolute length. The images were analyzed using ImageTool for Windows (version 3.00) (University of Texas Health Science Center in San Antonio), and the maximal width for each testis was determined. A minimum of 14 testes of each genotype was measured.

Bang Sensitivity Assay—For the bang sensitivity assay, flies were anesthetized with CO_2 and individually placed into 7-ml borosilicate glass scintillation vials (Thermo Fisher Scientific). Flies were allowed to recover from CO_2 for 2–3 h, and then each vial was vortexed (maximal setting) for 10 s, and the time for the fly to right itself and resume normal behavior was recorded. Any trial in which the fly remained stunned for >30 s was terminated and recorded as 30 s. A minimum of 20 flies was tested for any particular genotype.

Locomotor Assay—For each genotype, 20 5-day-old male flies were placed into an empty 10-cm plastic vial. With the top of the vial plugged, the vertical distance from the bottom of the vial to the top was 7 cm. After a 2-h period of recovery from CO_2 anesthesia, the vial was gently tapped once on the bench top to displace the flies to the bottom of the vial, and a digital camera recorded the movements of the flies for 6 s. Individual frames at 1-s intervals from 0 to 5 s were digitally captured and analyzed using ImageTool for Windows (version 3.00). The relative distance from the bottom of the vial for each fly at each time point was determined and used to obtain a mean distance for each group of flies at each time point. The assay was repeated for each genotype with a new cohort of male flies at least three times.

Electroretinograms (ERGs)—ERGs from flies immobilized with nail polish (Top Speed, Revlon) were recorded with a fine glass pipette filled with 3 M NaCl placed on the corneal surface of the fly's eye. The reference electrode was inserted into the thorax. Light flashes of 1 s were delivered from a 150-watt halogen lamp (Volpi), and field potential recordings were digitized and stored on a personal computer using Clampex software. At least two flies for each genotype were used to generate the ERG traces, and the amplitudes of the "on" and "off" transients as well as the sustained negative component were analyzed using Clampfit.

Larval NMJ Electrophysiology—Larval electrophysiological recordings and temperature control were performed as described (26). Modified HL3 contained 110 mM NaCl, 5 mM KCl, 10 mM $NaHCO_3$, 5 mM HEPES, 30 mM sucrose, 5 mM trehalose, and 20 mM $MgCl_2$ (pH 7.2), and $CaCl_2$ (concentrations indicated in Fig. 6). Excitatory junctional potential (EJP) recordings were made from muscles 6 or 7 using 90–110-megohm electrodes, and motor neurons were stimulated several times above threshold to ensure action potential initiation. For each animal, 60 EJPs were recorded, and the amplitudes were averaged to determine the individual EJP amplitude (observed failures at 0.25 mM Ca^{2+} were excluded). The mean EJP amplitude was determined from several animals (sample sizes indicated in bar graphs of Fig. 6).

Immunofluorescence Microscopy—Staining protocols were performed as described (27): anti-DLG (mouse; 4F3) was used at a dilution of 1:50. Anti-GluRIII/IIC was a gift from A. Di Antonio (Washington University, St. Louis, MO) and was used at a dilution of 1:1,000. Secondary antibodies tagged with Cy3 (Jackson ImmunoResearch Laboratories) or Alexa 488 (Molecular Probes) were used at 1:250. All fluorescent images were captured using a Zeiss 510 confocal microscope and processed using Amira 2.2 and ImageJ. Z stacks of synapses were acquired as delimited by DLG fluorescence. Using ImageJ, all three fluorescent channels of each Z stack were analyzed as two-dimensional projections of maximal fluorescence and quantitated as percentage of voxels in each Z stack that had a detectable signal above background. GluRIII/IIC and mitoGFP fluorescence were normalized to DLG fluorescence. Two Z stacks each from three individual animals (*i.e.* six total) for both wild type and $porin^{Rev8}$ were used for the analysis.

RESULTS

Generation of a Hypomorphic Mutant porin Allelic Series—A P element insertion allele of *porin* (Fig. 1*A*), $porin^{EY2333}$, was obtained from the *Drosophila* Gene Disruption Project (18). A series of hypomorphic alleles were derived from $porin^{EY2333}$ by imprecise P element excision (28). Long range PCR analysis of one of these excision alleles, $porin^{Rev8}$, revealed an insertion of ~7 kb in the *porin* locus (supplemental Fig. S1*C*), whereas PCR analysis of three other alleles demonstrate deletions involving the alternatively spliced 5′-untranslated exons and the first intron (supplemental Fig. S1, *A* and *B*). Sequence analysis of all alleles demonstrated intact coding exons. Western blot analysis of these alleles demonstrated severe reduction in Porin expression levels (Fig. 1*B* and supplemental Fig. S2). Based on the low residual amount of *porin* protein in $porin^{Rev8}$ mutants, this allele was chosen for further study.

porin Mutants Exhibit Partial Lethality and Reduced Viability—$porin^{Rev8}$ homozygous mutants are semilethal because significantly fewer than expected adult homozygotes

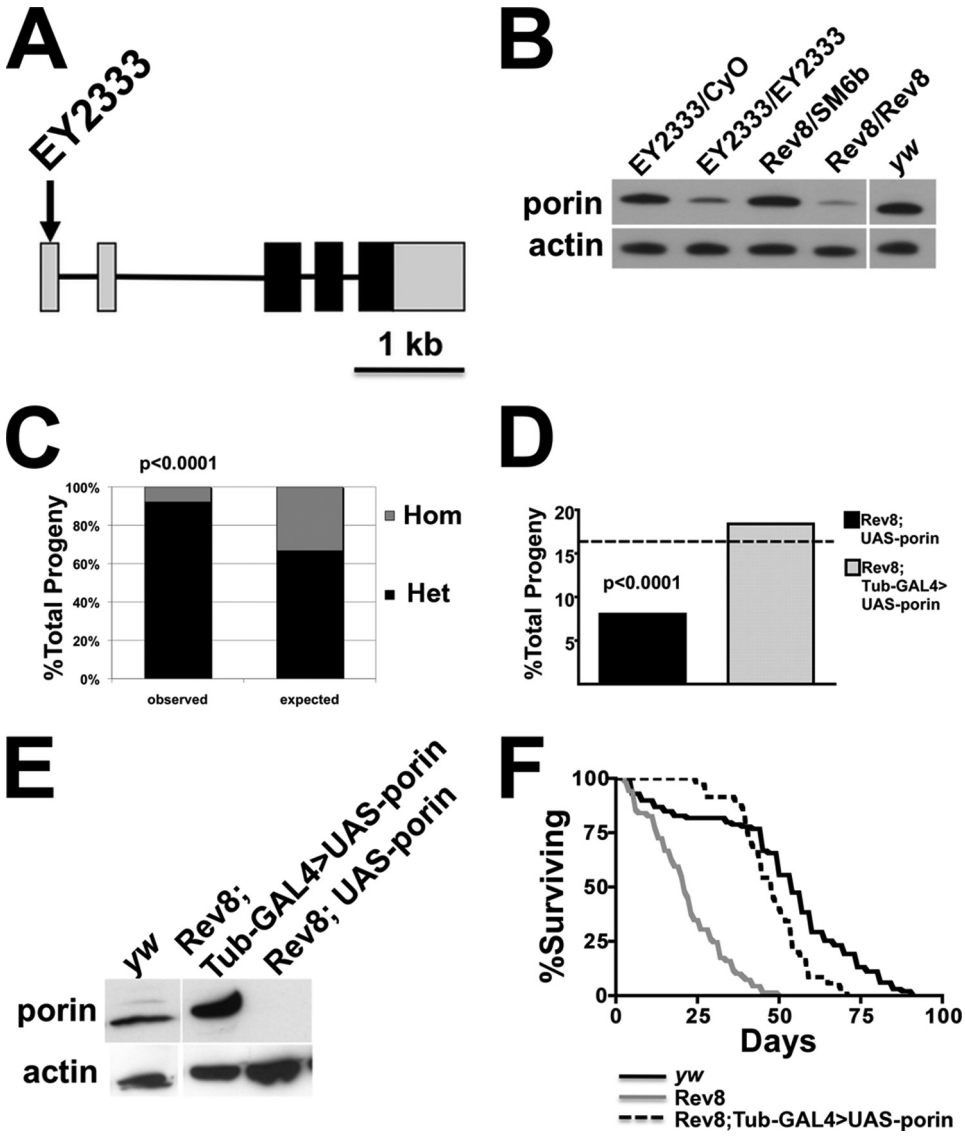

FIGURE 1. ***porin*-deficient flies exhibit partial developmental lethality and reduced lifespan.** *A*, the genomic organization of the *porin* locus is indicated in the *schematic*. The *arrow* indicates the insertion point of the P element in the *porin* gene. The *black boxes* indicate protein-coding exonic sequences, and the *gray boxes* indicate untranslated exonic regions (*UTR*). *B*, Western blot analysis of whole fly lysates of the indicated genotypes is shown. Blots were sequentially probed with Porin and actin antisera. *CyO* and *SM6b* are balancer chromosomes for chromosome 2 present in *porin* mutant heterozygotes. *C*, heterozygous *porin* mutant intercross was performed and the *porin* genotype of 457 adult F_1 progeny was inferred from the presence or absence of the balancer chromosome dominant marker. The *stacked bar graph* shows observed F_1 genotype proportions compared with the expected Mendelian ratio for wild type *porin*. *Hom*, $porin^{Rev8}/porin^{Rev8}$; *Het*, $porin^{Rev8}/SM6b$. *D*, a cross of *porin* mutant heterozygotes harboring either a wild type UAS-*porin* or *Tubulin-GAL4* (*Tub-GAL4*) (21) transgenes was performed. The bar graph shows the observed proportions of $porin^{Rev8}$ homozygotes harboring the UAS_*porin* transgene with or without the *Tubulin GAL4* driver (*Tub_GAL4*) (total number of F_1 progeny observed, 685). The *dashed line* indicates the expected frequency of both genotypes for wild type *porin*. Statistical significance for *C* and *D* was evaluated by Chi square analysis. *E*, a Western blot of whole-fly lysates of the indicated genotypes is shown to demonstrate restoration of *porin* levels by ectopic *porin* expression. *F*, survival curves for wild type (*yw*, $n = 99$), homozygous mutant ($porin^{Rev8}$, $n = 69$), and rescued homozygous mutant ($porin^{Rev8}$;*Tub-GAL4*>UAS-*porin*, $n = 35$) are shown. Rev8, $porin^{Rev8}$.

were observed (Fig. 1*C*). Homozygotes progress through embryogenesis and early larvogenesis, but ~75% fail to successfully transition from late larvogenesis to pupation and eclosion (data not shown). This partial lethality is specific to *porin* deficiency because homozygotes that ectopically express wild type *porin* are rescued into adulthood (Fig. 1, *D* and *E*). Adult $porin^{Rev8}$ homozygotes also exhibit reduced lifespans, and this phenotype is similarly rescued by ectopic *porin* expression (Fig. 1, *E* and *F*).

porin-deficient Mitochondria Exhibit Respiratory Defects—To examine the consequences of Porin deficiency on mitochondrial respiration, oxygen consumption in the presence of oxidizable substrates and ADP was measured from fresh mitochondria isolated from wild type and $porin^{Rev8}$ flies (Fig. 2*A* and supplemental Table S1). Mitochondria from $porin^{Rev8}$ mutants demonstrated a global respiratory defect, with significantly decreased ADP-stimulated oxygen consumption ("state III" respiration) in the presence of either complex I or II-dependent substrates. When activities of individual respiratory chain complexes were measured, *porin* mutants exhibited a significant partial deficiency of complex I activity (~30% of wild type activity) as well as an increase of complex III activity (~140% of wild type activity) (Fig. 2*B* and supplemental Table S2). These results demonstrate that in addition to decreased mitochondrial outer membrane permeability, Porin deficiency leads to perturbations in respiratory chain function and thus is valid a model for secondary respiratory chain deficiency.

porin Mutants Exhibit Defects of Fecundity and Fertility—Mutant *porin* flies have reduced fertility. $porin^{EY2333}$ male homozygotes are subfertile, whereas $porin^{Rev8}$ male homozygotes are absolutely infertile (no fertile cross has been observed after testing more than 1,000 individual $porin^{Rev8}$ males). This infertility is rescued by ectopic expression of *porin* cDNA in the testes using the *c135-GAL4* driver, which is expressed both in somatic cyst cells and spermatocytes (Fig. 3*A*) (23). Importantly, expression of other *Drosophila* VDAC isoforms present in the testis (CG17137 (*Porin2*) and CG17140) is not significantly altered in $porin^{Rev8}$ mutants (Fig. 3*A*). The other hypomorphic mutant *porin* alleles also demonstrate decreased fertility (supplemental Fig. S3*B*). Similar to the infertile mutant described by Oliva *et al.* (16), these mutants exhibit normal testes morphology, with normal appearing Nebenkern bodies by differential

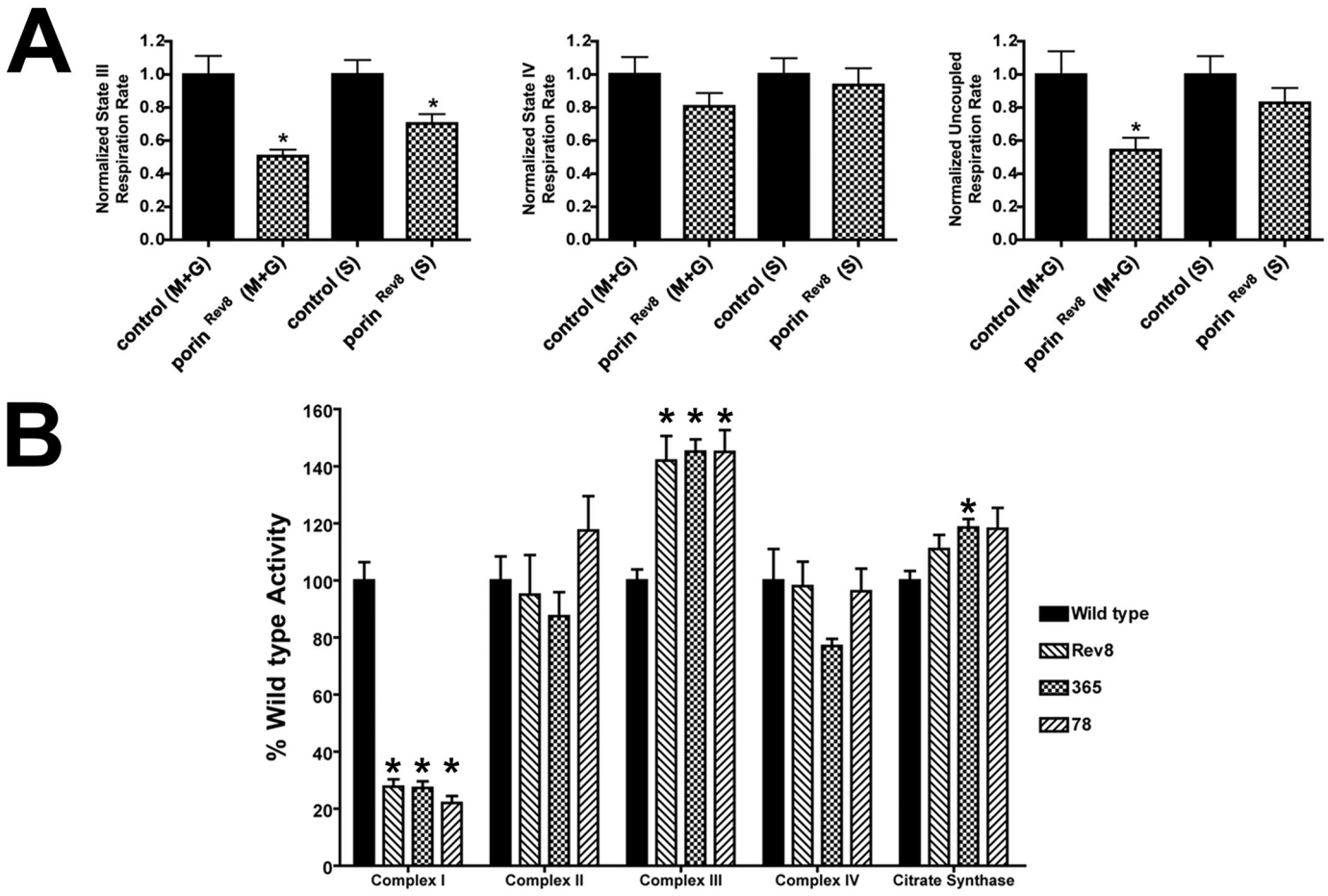

FIGURE 2. ***porin* mutants have defects of mitochondrial respiration and complex I activities.** *A*, normalized ADP-stimulated (*State III*), ADP-limiting (*State IV*), and uncoupled oxygen consumption rates of isolated mitochondria from control (*yw*) and $porin^{Rev8}$ flies are presented. The oxidizable substrates used in the assay were either malate and glutamate (*M*+*G*) or succinate (*S*). *, $p < 0.05$ by Student's *t* test with Welch correction. *B*, normalized activities from larval lysates of the individual respiratory chain complexes I–IV as well as citrate synthase are presented. *Wild type*, $porin^{Ex341}$; *Rev8*, $porin^{Rev8}$; *365*, $porin^{Ex365}$; *78*, $porin^{Ex78}$. *, $p < 0.001$ by Student's *t* test with Welch correction (*versus* wild type). *Error bars* represent S.E.

interference microscopy, yet they produce immotile sperm (data not shown). Further examination of dissected male reproductive tracts revealed that in $porin^{Rev8}$ male homozygotes the seminal vesicles are small and devoid of sperm, whereas the testes themselves are enlarged ~25% compared with wild type controls (Fig. 3*B*). In addition, although female $porin^{EY2333}$ homozygotes have normal fecundity and fertility, female $porin^{Rev8}$ homozygotes have severely reduced fecundity and fertility (Fig. 3*C*).

porin Mutants Demonstrate Neurological and Muscular Abnormalities—"Bang-sensitive" or stress-sensitive mutants are a phenotypic class of mutants that exhibit temporary paralysis when exposed to mechanical stress (29–32). This phenotype has been associated with mutations in genes involved in neuronal function as well as mitochondrial integrity (33–38). Two stress-sensitive mutants have been identified as nuclear-encoded mitochondrial genes: *stress sensitive B* (*sesB*), encoding the fly ortholog of the adenine nucleotide translocase (39), and *technical knock-out* (*tko*), encoding a subunit of the mitochondrial ribosome (40). Furthermore, mutations in the gene encoding Drp1, a protein involved in mitochondrial fission, also cause bang sensitivity (41). Analysis of mutant *porin* homozygotes revealed that these mutants also exhibit enhanced bang sensitivity, with hypomorphic $porin^{EY2333}$ homozygotes demonstrating a 2–3-fold increase in recovery time and imprecise excision mutant *porin* homozygotes showing at least a 6–7-fold increase in recovery time compared with wild type. Ectopic expression of wild type *porin* in the central nervous system (CNS) of mutant homozygotes rescues this abnormal phenotype (Fig. 4*A* and supplemental Fig. S3*A*). This defect is consistent with a defect in mitochondrial function.

In light of the pathological changes in muscle structure and function observed in $Vdac1^{-/-}$ mice (12) as well as in several *Drosophila* mutants that affect mitochondrial integrity (42–46), the possibility of muscle mitochondrial pathology and dysfunction was also examined. Electron microscopy of indirect flight skeletal muscle from 7-day-old flies revealed that mitochondria in *porin* mutant homozygotes appear larger than the wild type. Additionally, these mitochondria exhibit abnormal morphology, with regions of striking patterning of cristae (Fig. 4*C*). This abnormal morphology was not observed in age-matched control fly muscle (3.5 ± 0.4 mitochondrial inclusions per field (mean ± S.E.) for mutant; no inclusions were observed in wild type fields ($n = 8$ for wild type; $n = 15$ for mutant)). Interestingly, this

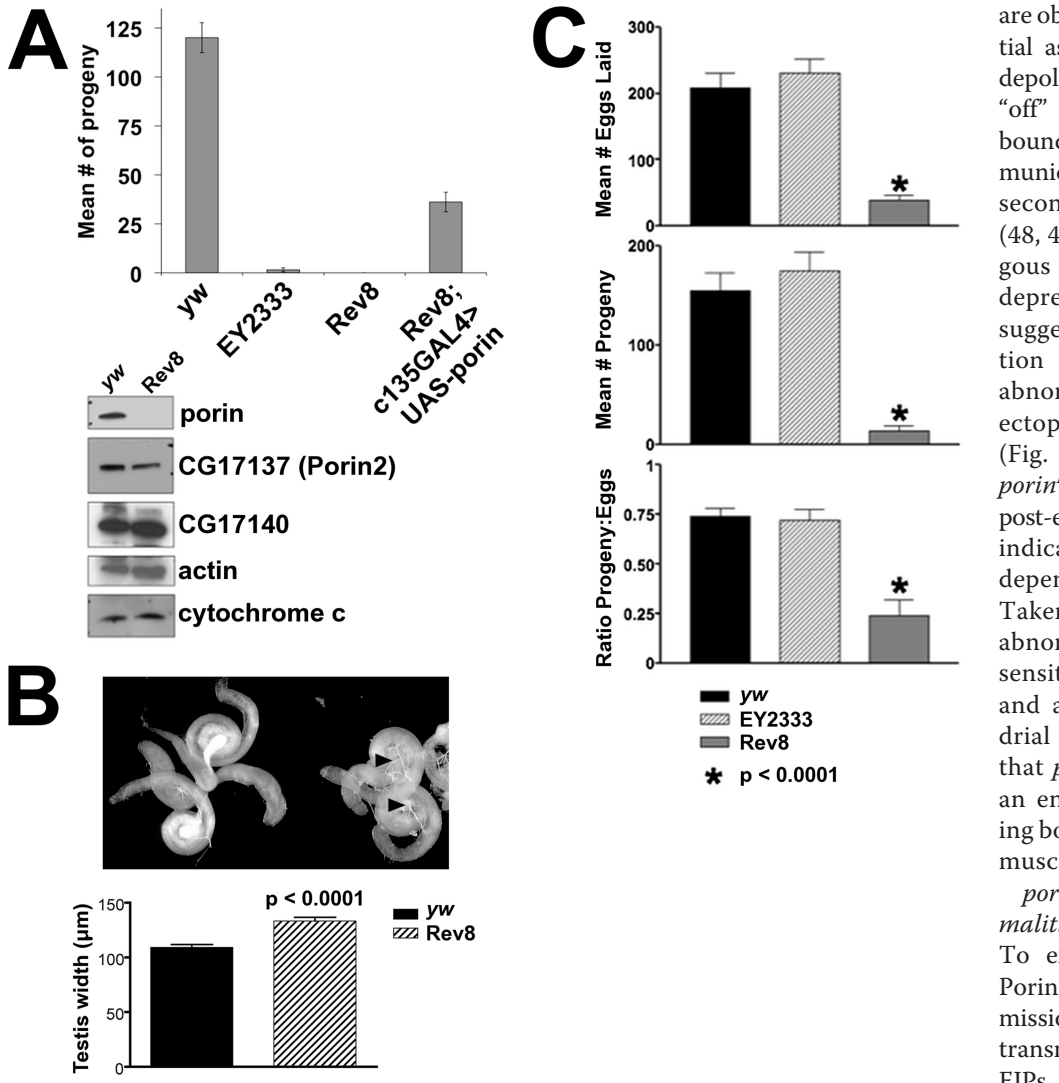

FIGURE 3. ***porin* hypomorphic mutant homozygotes are infertile/subfertile.** *A*, male fertility assay. *Bar graph* shows mean number of progeny observed from mating individual males of the indicated genotypes with *yw* virgin females. c135-*GAL4* is a *GAL4* driver that is expressed throughout the male reproductive tract (23). *Error bars* represent S.E. Sample sizes: *yw* ($n = 21$), $porin^{EY2333}$ ($n = 51$), $porin^{Rev8}$ ($n = 81$), rescued $porin^{Rev8}$ ($n = 74$). Western blot of testis lysates from males of the indicated genotypes is also shown. *B*, a representative dissected male reproductive tract is shown for *yw* (*right*) and $porin^{Rev8}$ (*left*). A *bar graph* indicating the mean greatest width of testes for both genotypes is shown below the picture. *Error bars* represent S.E. Sample sizes: yw ($n = 15$), $porin^{Rev8}$ ($n = 14$). *C*, Female fecundity/fertility assays. *Bar graphs* show mean number of eggs laid (*top*), mean number of adult progeny (*middle*), and mean ratio of progeny to eggs laid (*bottom*) observed for females of the indicated genotypes mated with *yw* males. Statistical significance evaluated by Student's *t* test with Welch correction (compared with *yw*). *Error bars* represent S.E. Sample sizes: *yw* ($n = 10$), $porin^{EY2333}$ ($n = 9$), and $porin^{Rev8}$ ($n = 9$). EY2333, $porin^{EY2333}$; Rev8, $porin^{Rev8}$.

abnormal cristae patterning appears very similar to recently described mitochondrial "swirls" that reportedly represent early stages of mitochondrial degeneration. These swirls are observed in flies as a function of aging and accumulate more rapidly when flies are reared in hyperoxic conditions (47). To grossly assess overall muscle function, normal locomotion of young adult control flies was quantified and compared with age-matched mutant flies (Fig. 4*B*). Homozygous mutant flies clearly exhibit a locomotor defect when compared with heterozygotes or wild type controls.

To further investigate potential CNS dysfunction in these mutants, electroretinograms were recorded from individual young and old flies. In a normal fly ERG, three potential changes are observed: the maintained potential associated with photoreceptor depolarization, and the "on" and "off" transients at the light/dark boundaries associated with communication between the retina and second order neurons (Fig. 5*A*) (48, 49). 3-week-old flies homozygous for $porin^{Rev8}$ demonstrate depression of all three potentials, suggesting a generalized dysfunction of the retina and CNS, an abnormality that is rescued by ectopic wild type *porin* expression (Fig. 5*B*). Interestingly, young $porin^{Rev8}$ mutant flies (2–3 days post-eclosion) exhibit normal ERGs, indicating a progressive and age-dependent pathology (Fig. 5*C*). Taken together, the observed ERG abnormalities, increased bang sensitivity, defective locomotion, and abnormal muscle mitochondrial morphology demonstrate that *porin*-deficient flies manifest an encephalomyopathy, comprising both primary CNS and primary muscle pathology.

porin Mutants Exhibit Abnormalities of Synaptic Transmission—To examine the consequence of Porin deficiency on synaptic transmission, we evaluated basal neurotransmitter release by recording EJPs at the larval neuromuscular junction (NMJ) (Fig. 6). When stimulated at 1 Hz in a bath containing 1 mM Ca^{2+}, there was no significant difference in mean EJP amplitude between wild type and $porin^{Rev8}$ mutants (Fig. 6*B*). However, when the experiment was performed in the presence of low extracellular Ca^{2+} (0.25 mM), a significant increase in EJP amplitude was observed for $porin^{Rev8}$ compared with controls (Fig. 6*C*). In addition, wild type controls on average failed to evoke EJPs in 24% of the stimulations, whereas $porin^{Rev8}$ larvae only failed at a mean frequency of 7% in 0.25 mM extracellular Ca^{2+} (Fig. 6*D*). We also recorded spontaneous synaptic ("mini") release events (mEJPs) in the presence of tetrodotoxin and 0.5 mM extracellular Ca^{2+} and analyzed all events with an mEJP amplitude >0.4 mV. Comparing wild type to Porin-deficient mutants, we did not observe any significant difference in mEJP amplitude, frequency, or distribution, indicating no gross difference in synaptic vesicular size or number (Fig. 6, *E* and *F*). Taken together, these observations indicate that Porin-deficient mutants exhibit a subtle increase in the

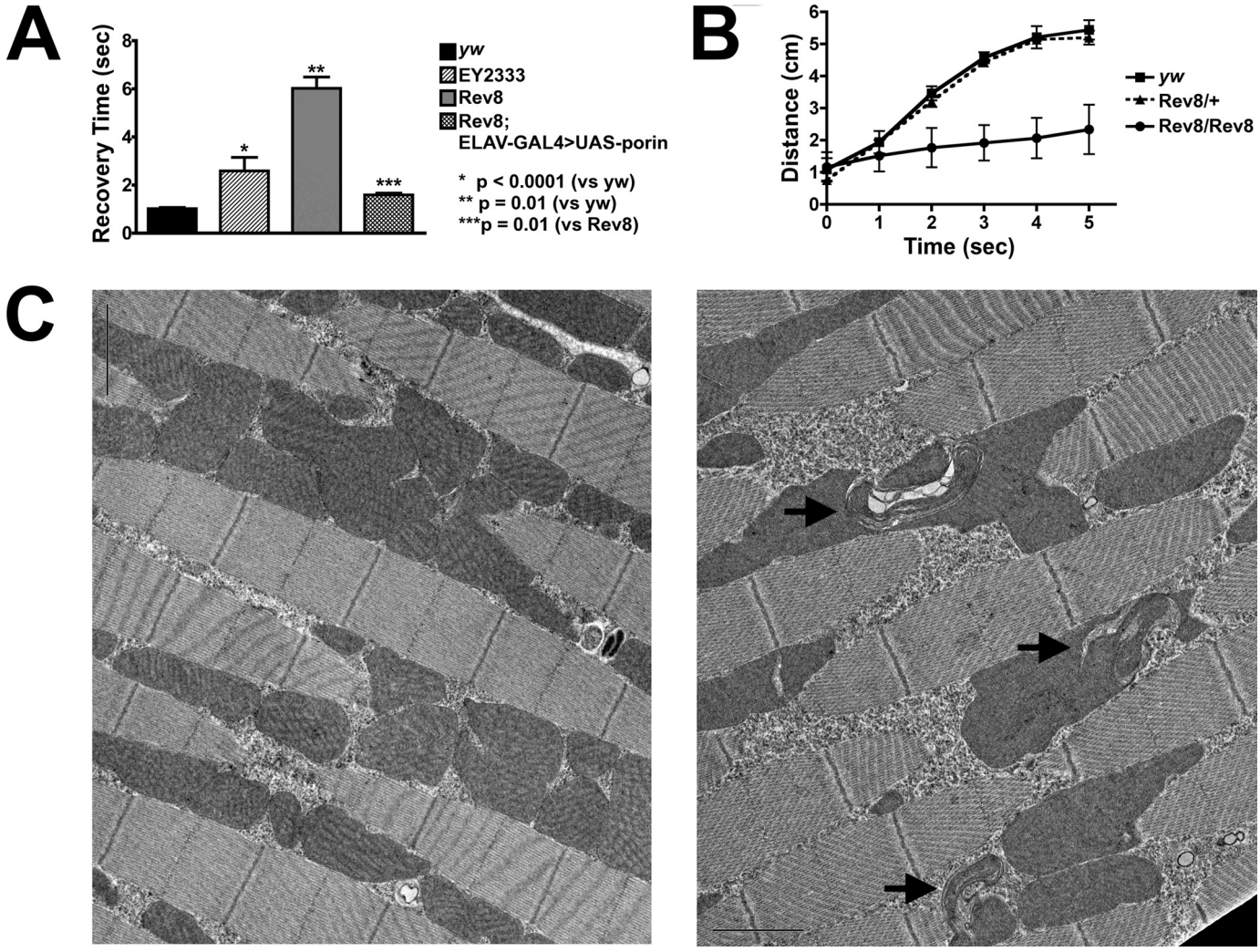

FIGURE 4. ***porin* mutants demonstrate neurologic dysfunction and abnormal muscle mitochondria.** *A*, bang sensitivity assay. The mean recovery time in seconds for each of the indicated genotypes is depicted. *ELAV-GAL4* is a CNS-specific *GAL4* driver (22). The *error bars* represent S.E. Statistical significance was evaluated by the Student's *t* test with Welch correction. Sample size for each genotype: *yw* ($n = 50$); $porin^{EY2333}$ homozygotes ($n = 20$); $porin^{Rev8}$ homozygotes ($n = 93$); and rescued $porin^{Rev8}$ homozygotes ($n = 78$). *B*, locomotion assay. *Graph* depicts distance traveled from bottom of vial over time for flies of the indicated genotypes. Each data point represents the average median distance for a population of 20 males. The *error bars* represent one S.D. for three to four replicates. EY2333, $porin^{EY2333}$; Rev8, $porin^{Rev8}$. *C*, a representative EM section from indirect flight muscle for wild type (*left*) and mutant (*right*) is shown. The *black arrows* in the mutant EM section indicate mitochondria with abnormal cristae.

release of neurotransmitters at the NMJ under conditions of low release probability.

porin Mutants Exhibit Abnormal Distribution of Mitochondria in Motor Neurons—Given the observed mitochondrial and neuromuscular dysfunction, we also examined the distribution of mitochondria in motor neurons by expressing mitochondrial-targeted GFP (mitoGFP) in larval motor neurons using the UAS/*GAL4* system with a *GAL4* driver that is specifically expressed in motor neurons (50). When examining the NMJ by immunofluorescence, there is no observable difference in staining for the synaptic marker Dlg (51) or for the post-synaptic glutamate receptor (GluRIII/IIC) (52); however, there is an ~70% reduction in mitoGFP fluorescence when comparing wild type to $porin^{Rev8}$ mutants (Fig. 7, *A* and *B*). When mitoGFP fluorescence is examined at the level of the ventral nerve cord in controls, mitoGFP predominantly localizes to the branching motor axons and motor neuron projections in the neuropil (Fig. 7*C*). In contrast, the $porin^{Rev8}$ mutant appears to have reduced mitoGFP in the neuropil and motor axon, with increased punctate clusters in the motor neuron cell bodies bordering the ventral nerve cord (Fig. 7*C*). These observations of abnormal mitochondrial distribution suggest that porin deficient mutants exhibit abnormal neuronal mitochondrial trafficking.

DISCUSSION

These studies demonstrate that deficiency of *porin* in *Drosophila* causes a wide range of phenotypes that are remarkably reminiscent of mutant phenotypes seen in VDAC-deficient mice. Flies mutant for *porin* exhibit a partial developmental lethality, similar to mice deficient for *Vdac1* that manifest variable partial embryonic lethality depending on the genetic background (11). Both *porin* mutant flies and VDAC mutant mouse embryonic stem cells exhibit reductions in coupled mitochondrial respiration associated with secondary partial respiratory chain deficiencies (53).

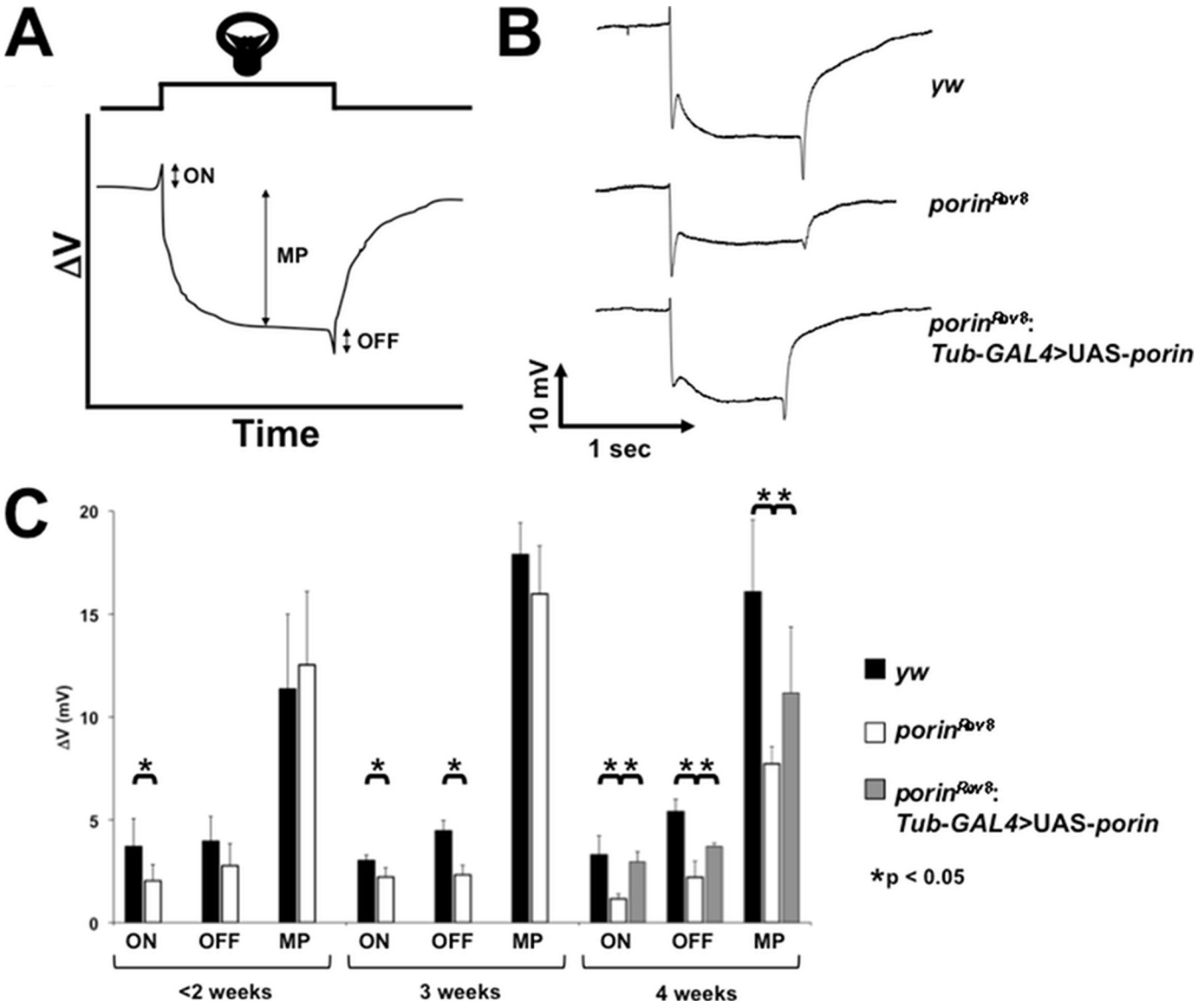

FIGURE 5. ***porin* homozygous mutants exhibit abnormal ERGs.** *A*, stereotypical "wild type" ERG are depicted. On-transient (*ON*), off-transient (*OFF*), and maintained potentials (*MP*) evidenced during light pulse are indicated. *B*, representative ERGs for wild type (*yw*), homozygous mutant (*porin*^{Rev8}), and rescue homozygous mutant (*porin*^{Rev8}; *Tub-GAL4*>UAS_*porin*) are shown to the *right*. *C*, *bar graph* depicts mean potentials (+S.E.) for each genotype. Statistical significance was evaluated by the Student's *t* test with Welch correction. Sample size for each genotype: *yw* ($n = 3$); *porin*^{Rev8} homozygotes ($n = 5$); and rescued *porin*^{Rev8} homozygotes ($n = 3$).

Whereas mice deficient for *Vdac1* and/or *Vdac3* have learning deficits and electrophysiological abnormalities of synaptic plasticity in the hippocampus (11), mutant flies have CNS dysfunction as demonstrated by enhanced bang sensitivity and electrophysiological abnormalities evident at both the NMJ and the retina. Both *porin*-deficient flies and *Vdac1*-null mice have enlarged abnormal mitochondria in skeletal muscle (12). In addition, mutant flies show locomotor problems, whereas mice with severely reduced VDAC (*Vdac1/3*$^{-/-}$) have marked exercise intolerance (54). Finally, male hypomorphic *porin* mutants are infertile with immotile sperm, whereas *Vdac3* deficient male mice are infertile from a sperm motility defect (13). The remarkable similarity of mutant phenotypes in the fly and mouse suggest that VDAC function is conserved among higher eukaryotes and validates *Drosophila* as a genetic model system to study VDAC regulation and function.

To date, no VDAC mutations in humans have been reported. One prior case report described an infant with hypotonia and developmental delay that demonstrated reduced *in vitro* substrate oxidation in mitochondria isolated from skeletal muscle and reduced VDAC by Western blot analysis of skeletal muscle mitochondria and fibroblasts (55). However, a DNA mutation for this patient has not been reported, and thus, the reduction in VDAC may represent a secondary phenomenon. Therefore, at this time, abnormalities of VDAC have not been established convincingly as a cause of human mitochondrial encephalomyopathy. However, the observed mutant phenotypes of fruit flies and mice deficient for VDAC, including the presence of secondary respiratory chain deficiencies, suggest

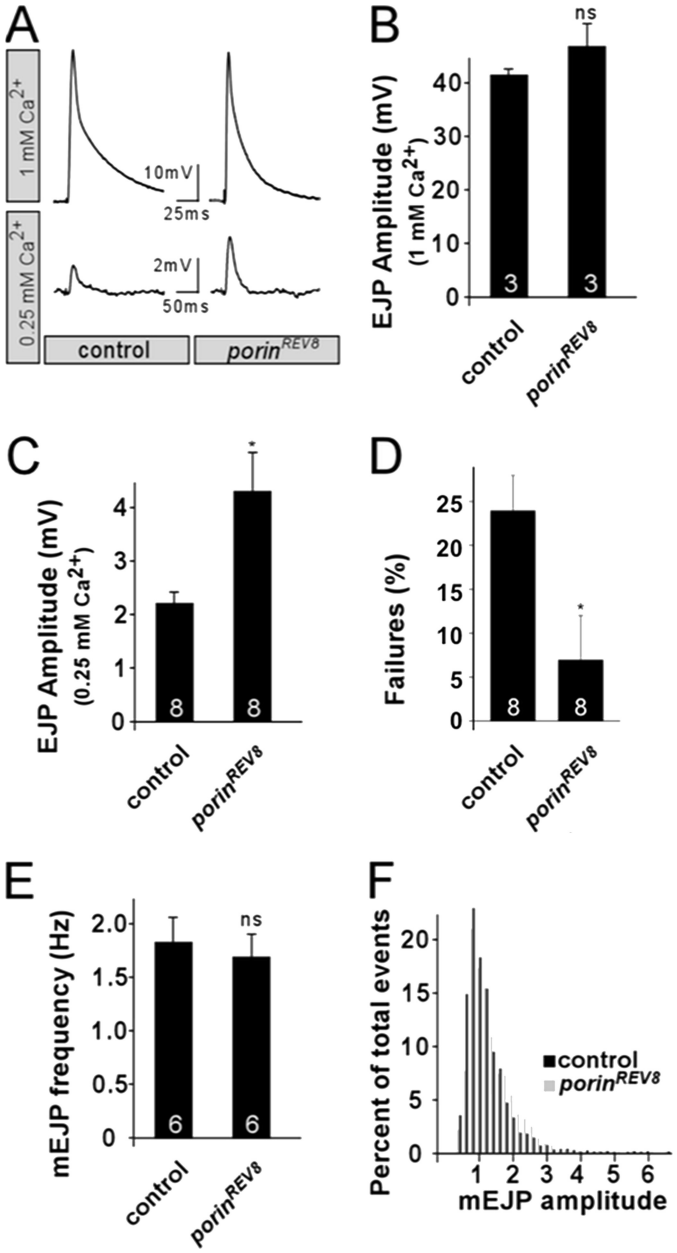

FIGURE 6. **Abnormal NMJ neurotransmission in *porin* mutants.** *A*, representative EJP traces recorded at 1 Hz at the indicated extracellular Ca^{2+} concentrations for both control (*yw*) and $porin^{Rev8}$ animals. *B* and *C*, mean EJP amplitudes recorded at 1 Hz at 1 mM Ca^{2+} in *B* or 0.25 mM Ca^{2+} in *C*. *D*, percentage of stimulations that failed to evoke EJP at 0.25 mM Ca^{2+}. *E* and *F*, spontaneous release events (*mEJPs*) were recorded for both control (*yw*) and $porin^{Rev8}$ animals and expressed as quantification of mEJP frequency in *E* and amplitude distribution in *F*. Statistical significance was evaluated by Student's *t* test. *, $p < 0.05$, *ns*, not significant.

that VDAC deficiency may be an unrecognized cause of human mitochondrial encephalomyopathy and that the study of VDAC deficiency in model systems should provide insights into the pathophysiology of mitochondrial disease and potential therapeutic approaches.

Although the hypomorphic alleles $porin^{Rev8}$, $porin^{Ex365}$, and $porin^{Ex78}$ demonstrate similar gross expression (supplemental Fig. S2) and biochemical phenotypes (Fig. 2), the *porin* mutants demonstrate a spectrum of severity for the bang sensitivity and male fertility mutant phenotypes, with $porin^{Ex78}$ showing milder phenotypes compared with $porin^{Ex365}$ and $porin^{Rev8}$ (supplemental Fig. S3). These abnormal phenotypes are caused by deficiency of Porin because ectopic expression of wild type *porin* in $porin^{Rev8}$, the most severe mutant, is sufficient to rescue the mutant phenotypes (Figs. 3*A* and 4*A*). The mechanism for this observed variable expressivity is not currently understood and requires further investigation. One possibility is that because these alleles differentially involve the 5′-untranslated exons and introns upstream from the *porin*-coding sequence (supplemental Fig. S1), they may have different effects on the cellular expression patterns for *porin* in the brain and in the testes that fall below the sensitivity of the Western blot analyses employed for this study.

Male infertility in *Drosophila* caused by mutations in genes affecting mitochondrial function and/or morphology other than *porin* has been reported previously. These include mutations in components of the respiratory chain, such as *bellwether* (α subunit of the mitochondrial ATP synthase) (56) and *cyt-c-d* (cytochrome *c*) (57), as well as genes that regulate mitochondrial fission/fusion such as *fuzzy onion* (*fzo*) (44) and *Rhomboid-7* (58). Whether the mechanism of male infertility in *porin* mutant homozygotes is related to a sperm flagellar structural defect, as seen in $Vdac3^{-/-}$ mice (13), a defect in spermatid individualization, as seen with *cyt-c-d* mutants (57), and/or a deficiency in mitochondrial ATP production or mitochondrial dynamics contributing to sperm immotility remains to be determined.

A previous report suggested that expression of *porin* and *CG17137* (*Porin2*) is coordinately regulated based on a failure to detect *Porin2* messenger RNA in pupa homozygous for a P element inserted in intron 1 of *porin* ($porin^{l(2)k08405}$) downstream of $porin^{EY2333}$ (59). The authors also hypothesized that the male infertility phenotype could be due to absence of *Porin2* expression. In contrast, as demonstrated in this report, *Porin2* expression in $porin^{Rev8}$ testes is not significantly altered by Western analysis and the infertility phenotype in *porin* mutants is rescued by ectopic expression of *porin* wild type cDNA in mutant testes (Fig. 3*A*). These data suggest that the male infertility phenotype in *porin* hypomorphic mutants is due entirely to loss of *porin* expression. However, the possibility that $porin^{Rev8}$ and $porin^{l(2)k08405}$ differentially affect expression of *Porin2* cannot be formally excluded.

Although the mechanism of abnormal neuronal mitochondrial distribution secondary to Porin deficiency remains to be determined, the electrophysiological and mitochondrial defects observed at the NMJ in *porin*-deficient mutants is very similar to the phenotype observed in *drp1* mutants (41). DRP1, dynamin-related protein, is a GTPase that is a central component of the mitochondrial outer membrane fission machinery involved in regulating mitochondrial dynamics (60). It was also recently reported that pharmacological inhibition of complex I activity in *Drosophila* larvae significantly reduces presynaptic anterograde trafficking of mitochondria (61). Mitochondria isolated from *porin*-deficient flies demonstrate a significant reduction in complex I activity (Fig. 2*B*). In addition, it has recently been demonstrated that the mitochondrial protein Miro inhibits kinesin-mediated anterograde transport of neuronal mito-

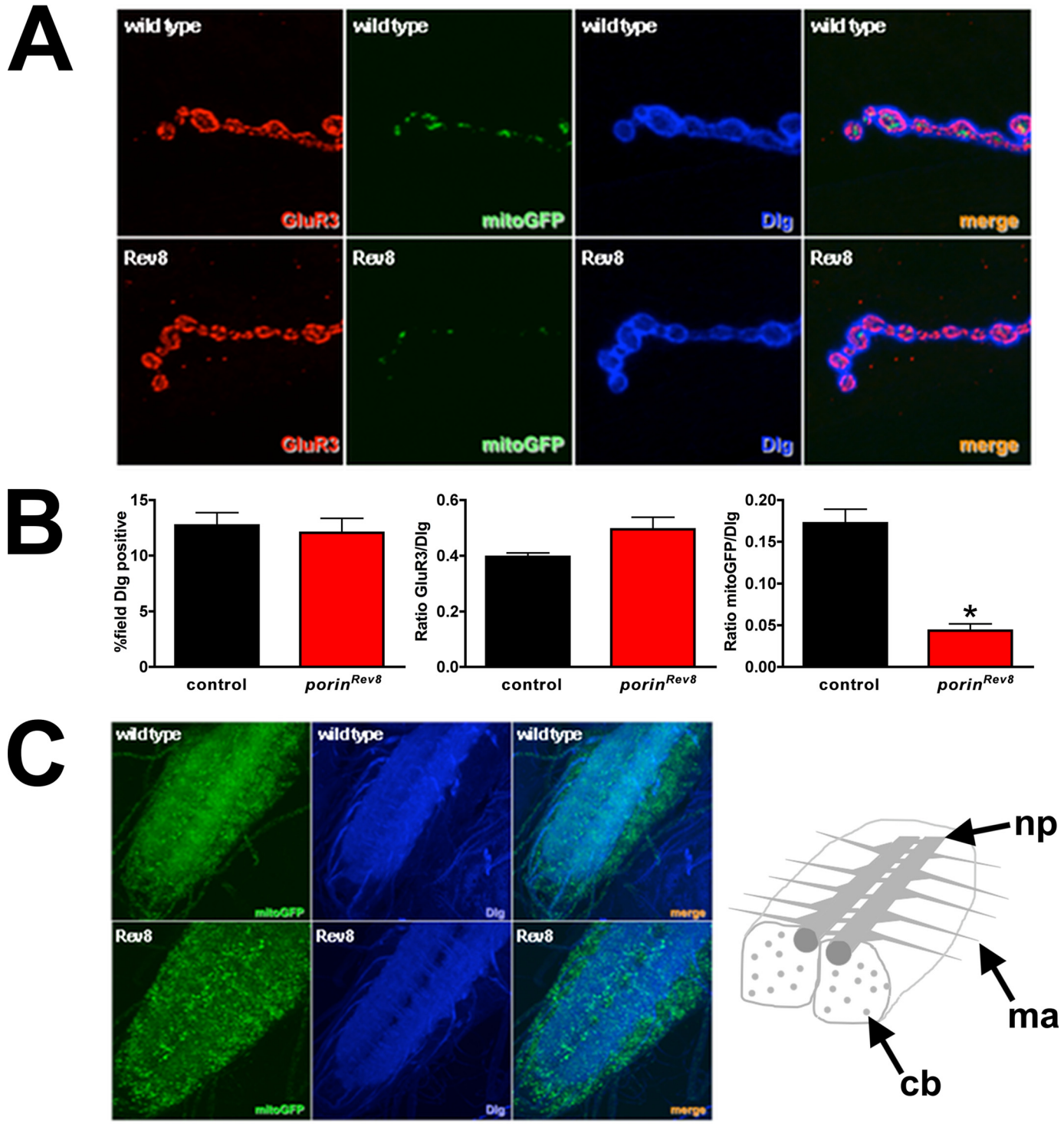

FIGURE 7. **porin mutants have reduced mitochondria in NMJ presynaptic termini.** *A*, labeling of third instar larval NMJs with Dlg (*blue*) to outline boutons, GluR3 (GluRIII/IIC, *red*) to demarcate postsynaptic receptor field, and mitoGFP (*green*) expressed in motor neurons. *B*, quantification of fluorescence per field demonstrates decreased mitochondria in *porin*^{Rev8}. *Error bars* represent S.E. *, $p < 0.05$ by Student's *t* test with Welch correction. *C*, third instar larval ventral nerve cords labeled with Dlg (*blue*), which labels the neuropil (*np*) and motor axons (*ma*), and with mitoGFP (*green*). In *porin*^{Rev8} animals, mitoGFP is more prominent in the cell bodies (*cb*) and sparser in the neuropil and motor axons compared with wild type (*yw*). Rev8, *porin*^{Rev8}.

chondria in a Ca^{2+}-dependent manner (62). Given that the NMJ phenotypes of *porin* and *drp1* mutants are similar and that presynaptic resting Ca^{2+} levels are elevated in *drp1* mutants (41), it is possible that presynaptic Ca^{2+} levels in *porin* mutants are elevated, resulting in Miro-dependent inhibition of mitochondrial anterograde transport. Further studies are required to address whether disruption of a possible direct or indirect interaction with Drp1, mitochondrial complex I deficiency with mitochondrial depolarization, and/or perturbations in presynaptic Ca^{2+} homeostasis con-

tribute to abnormal neuronal distribution of mitochondria in *porin* mutants.

Acknowledgments—We acknowledge Hugo Bellen for generous support and insightful comments and suggestions. We thank Yi Zhou for technical assistance in generating transmission electron microscopy images of indirect flight muscle. We acknowledge Yuchun He for performing the embryo injections to generate UAS_porin transgenic flies and Yan Huang for technical molecular biology assistance.

REFERENCES

1. Sorgato, M. C., and Moran, O. (1993) *Crit. Rev. Biochem. Mol. Biol.* **28,** 127–171
2. Blachly-Dyson, E., Song, J., Wolfgang, W. J., Colombini, M., and Forte, M. (1997) *Mol. Cell Biol.* **17,** 5727–5738
3. Sampson, M. J., Lovell, R. S., and Craigen, W. J. (1997) *J. Biol. Chem.* **272,** 18966–18973
4. Blachly-Dyson, E., Zambronicz, E. B., Yu, W. H., Adams, V., McCabe, E. R., Adelman, J., Colombini, M., and Forte, M. (1993) *J. Biol. Chem.* **268,** 1835–1841
5. Rahmani, Z., Maunoury, C., and Siddiqui, A. (1998) *Eur. J. Hum. Genet.* **6,** 337–340
6. Rostovtseva, T., and Colombini, M. (1996) *J. Biol. Chem.* **271,** 28006–28008
7. Komarov, A. G., Graham, B. H., Craigen, W. J., and Colombini, M. (2004) *Biophys. J.* **86(1 Pt 1),** 152–162
8. Shimizu, S., Narita, M., and Tsujimoto, Y. (1999) *Nature* **399,** 483–487
9. Cheng, E. H., Sheiko, T. V., Fisher, J. K., Craigen, W. J., and Korsmeyer, S. J. (2003) *Science* **301,** 513–517
10. Gincel, D., Zaid, H., and Shoshan-Barmatz, V. (2001) *Biochem. J.* **358,** 147–155
11. Weeber, E. J., Levy, M., Sampson, M. J., Anflous, K., Armstrong, D. L., Brown, S. E., Sweatt, J. D., and Craigen, W. J. (2002) *J. Biol. Chem.* **277,** 18891–18897
12. Anflous, K., Armstrong, D. D., and Craigen, W. J. (2001) *J. Biol. Chem.* **276,** 1954–1960
13. Sampson, M. J., Decker, W. K., Beaudet, A. L., Ruitenbeek, W., Armstrong, D., Hicks, M. J., and Craigen, W. J. (2001) *J. Biol. Chem.* **276,** 39206–39212
14. Messina, A., Neri, M., Perosa, F., Caggese, C., Marino, M., Caizzi, R., and De Pinto, V. (1996) *FEBS Lett.* **384,** 9–13
15. Ryerse, J., Blachly-Dyson, E., Forte, M., and Nagel, B. (1997) *Biochim. Biophys. Acta* **1327,** 204–212
16. Oliva, M., De Pinto, V., Barsanti, P., and Caggese, C. (2002) *Mol. Genet. Genomics* **267,** 746–756
17. Graham, B. H., and Craigen, W. J. (2005) *Mol. Genet. Metab.* **85,** 308–317
18. Bellen, H. J., Levis, R. W., Liao, G., He, Y., Carlson, J. W., Tsang, G., Evans-Holm, M., Hiesinger, P. R., Schulze, K. L., Rubin, G. M., Hoskins, R. A., and Spradling, A. C. (2004) *Genetics* **167,** 761–781
19. Spradling, A. C., Stern, D., Beaton, A., Rhem, E. J., Laverty, T., Mozden, N., Misra, S., and Rubin, G. M. (1999) *Genetics* **153,** 135–177
20. Brand, A. H., and Perrimon, N. (1993) *Development* **118,** 401–415
21. Lee, T., and Luo, L. (1999) *Neuron* **22,** 451–461
22. Lin, D. M., and Goodman, C. S. (1994) *Neuron* **13,** 507–523
23. Hrdlicka, L., Gibson, M., Kiger, A., Micchelli, C., Schober, M., Schöck, F., and Perrimon, N. (2002) *Genesis* **34,** 51–57
24. Trounce, I. A., Kim, Y. L., Jun, A. S., and Wallace, D. C. (1996) *Methods Enzymol.* **264,** 484–509
25. Verstreken, P., Koh, T. W., Schulze, K. L., Zhai, R. G., Hiesinger, P. R., Zhou, Y., Mehta, S. Q., Cao, Y., Roos, J., and Bellen, H. J. (2003) *Neuron* **40,** 733–748
26. Koh, T. W., Verstreken, P., and Bellen, H. J. (2004) *Neuron* **43,** 193–205
27. Bellen, H. J., and Budnik, V. (2000) in *Drosophila Protocols* (Sullivan, M., Ashburner, M., and Hawley, R. S., eds) pp. 175–199, CSHL Press, Cold Spring Harbor, New York
28. Robertson, H. M., Preston, C. R., Phillis, R. W., Johnson-Schlitz, D. M., Benz, W. K., and Engels, W. R. (1988) *Genetics* **118,** 461–470
29. Benzer, S. (1971) *Jama* **218,** 1015–1022
30. Homyk, T., Jr. (1977) *Genetics* **87,** 105–128
31. Homyk, T., Jr., Szidonya, J., and Suzuki, D. T. (1980) *Mol. Gen. Genet.* **177,** 553–565
32. Ganetzky, B., and Wu, C. F. (1982) *J. Neurophysiol.* **47,** 501–514
33. Ramaswami, M., and Tanouye, M. A. (1989) *Proc. Natl. Acad. Sci. U.S.A.* **86,** 2079–2082
34. Pavlidis, P., Ramaswami, M., and Tanouye, M. A. (1994) *Cell* **79,** 23–33
35. Schubiger, M., Feng, Y., Fambrough, D. M., and Palka, J. (1994) *Neuron* **12,** 373–381
36. Kuebler, D., and Tanouye, M. A. (2000) *J. Neurophysiol.* **83,** 998–1009
37. Lee, J., and Wu, C. F. (2002) *J. Neurosci.* **22,** 11065–11079
38. Trotta, N., Rodesch, C. K., Fergestad, T., and Broadie, K. (2004) *J. Neurobiol.* **60,** 328–347
39. Zhang, Y. Q., Roote, J., Brogna, S., Davis, A. W., Barbash, D. A., Nash, D., and Ashburner, M. (1999) *Genetics* **153,** 891–903
40. Royden, C. S., Pirrotta, V., and Jan, L. Y. (1987) *Cell* **51,** 165–173
41. Verstreken, P., Ly, C. V., Venken, K. J., Koh, T. W., Zhou, Y., and Bellen, H. J. (2005) *Neuron* **47,** 365–378
42. Clark, I. E., Dodson, M. W., Jiang, C., Cao, J. H., Huh, J. R., Seol, J. H., Yoo, S. J., Hay, B. A., and Guo, M. (2006) *Nature* **441,** 1162–1166
43. Greene, J. C., Whitworth, A. J., Kuo, I., Andrews, L. A., Feany, M. B., and Pallanck, L. J. (2003) *Proc. Natl. Acad. Sci. U.S.A.* **100,** 4078–4083
44. Hales, K. G., and Fuller, M. T. (1997) *Cell* **90,** 121–129
45. Xu, Y., Condell, M., Plesken, H., Edelman-Novemsky, I., Ma, J., Ren, M., and Schlame, M. (2006) *Proc. Natl. Acad. Sci. U.S.A.* **103,** 11584–11588
46. Yarosh, W., Monserrate, J., Tong, J. J., Tse, S., Le, P. K., Nguyen, K., Brachmann, C. B., Wallace, D. C., and Huang, T. (2008) *PLoS Genet.* **4,** e6
47. Walker, D. W., and Benzer, S. (2004) *Proc. Natl. Acad. Sci. U.S.A.* **101,** 10290–10295
48. Pak, W. L. (1995) *Invest. Ophthalmol. Vis. Sci.* **36,** 2340–2357
49. Lo, M. V., and Pak, W. L. (1981) *J. Gen. Physiol.* **77,** 155–175
50. Yeh, E., Gustafson, K., and Boulianne, G. L. (1995) *Proc. Natl. Acad. Sci. U.S.A.* **92,** 7036–7040
51. Parnas, D., Haghighi, A. P., Fetter, R. D., Kim, S. W., and Goodman, C. S. (2001) *Neuron* **32,** 415–424
52. Marrus, S. B., Portman, S. L., Allen, M. J., Moffat, K. G., and DiAntonio, A. (2004) *J. Neurosci.* **24,** 1406–1415
53. Wu, S., Sampson, M. J., Decker, W. K., and Craigen, W. J. (1999) *Biochim. Biophys. Acta* **1452,** 68–78
54. Anflous-Pharayra, K., Cai, Z. J., and Craigen, W. J. (2007) *Biochim. Biophys. Acta* **1767,** 136–142
55. Huizing, M., Ruitenbeek, W., Thinnes, F. P., DePinto, V., Wendel, U., Trijbels, F. J., Smit, L. M., ter Laak, H. J., and van den Heuvel, L. P. (1996) *Pediatr. Res.* **39,** 760–765
56. Jacobs, H., Stratmann, R., and Lehner, C. (1998) *Mol. Gen. Genet.* **259,** 383–387
57. Arama, E., Bader, M., Srivastava, M., Bergmann, A., and Steller, H. (2006) *EMBO J.* **25,** 232–243
58. McQuibban, G. A., Lee, J. R., Zheng, L., Juusola, M., and Freeman, M. (2006) *Curr. Biol.* **16,** 982–989
59. Guarino, F., Specchia, V., Zapparoli, G., Messina, A., Aiello, R., Bozzetti, M. P., and De Pinto, V. (2006) *Biochem. Biophys. Res. Commun.* **346,** 665–670
60. Santel, A., and Frank, S. (2008) *IUBMB Life* **60,** 448–455
61. Tong, J. J. (2007) *Biol. Bull* **212,** 169–175
62. Wang, X., and Schwarz, T. L. (2009) *Cell* **136,** 163–174